International Journal of Mechanical, Industrial and Aerospace Sciences
ISSN: 2517-9950
Vol:5, No:8, 2011

Effect of Including Thermal Process on Spot Welded and Weld-Bonded Joints

Essam A. Al-Bahkali

Abstract**—**A three-dimensional finite element modeling for austenitic stainless steel AISI 304 annealed condition sheets of 1.0 mm thickness are developed using ABAQUS® software. This includes spot welded and weld bonded joints models. Both models undergo thermal heat caused by spot welding process and then are subjected to axial load up to the failure point. The properties of elastic and plastic regions, modulus of elasticity, fracture limit, nugget and heat affected zones are determined. Complete load-displacement curve for each joining model is obtained and compared with the experiment data and with the finite element models without including the effect of thermal process. In general, the results obtained for both spot welded and weld-bonded joints affected by thermal process showed an excellent agreement with the experimental data.

Keywords**—**Heat Affected Zone, Spot Welded, Thermal Process, Weld-Bonded.

I. Introduction

RESISTANCE Spot Welding (RSW) was discovered accidently by E. Thomson in 1877 during the process of short circuit [1]. This type of welding was used in small scale until the mid of twenty century when RSW became extensively used in manufacturing industry such as automotive and aerospace for joining metal sheets. The process for joining metal sheets can be done by applying opposing forces using the electrodes tips. These forces are applied before, during and after the application of current to hold the contact area at the weld interfaces. The current and the heat generation are localized as a result of the contact area of the electrodes tips. These contact area can be used to defined the weld nugget size.

Weld-bonded is a combination of resistance spot welding and adhesive bonding, which has gathered wide acceptance as an effective joining process for significant improvement in static, dynamic and impact toughness properties of sheet metal joints. It also improves the corrosion, noise resistance, and joint stiffness. Craddock [2] discovered that as early as 1966 the Soviet Union used resistance weld-bonding process as the primary means of fastening for their designed aircraft.

In order to reach an optimum welding quality of a spot welded or a weld-bonded joints, different calibration trials have to be conducted to setup the optimum welding parameters, i.e. welding current, electrode force, and welding time [3], [4].

Essam. A. Al-Bahkali is with the Mechanical Engineering Department, King Saud University, P.O. Box 800, Riyadh 11421, Saudi Arabia (phone: +9661-467-6675; fax: +9661-467-6652; e-mail: ebahkali@ ksu.edu.sa).

In predicting stress distribution, stress concentration and failure modes of a weld-bonded or a spot welded nugget, finite element (FE) modeling was employed. Two separate spot welding and adhesive bonding FE models were utilized in predicting the behavior of a weld-bonded joint by Cavalli et al. [5]. Furthermore, Cryns [6] claimed that peel and tensile strengths, in weld bonded structures, are higher than adhesive or spot welded ones.

Most researchers concentrated on two dimensional FE modeling procedures to investigate RSW problems. Chang et al. [7] used a three dimensional elasto-plastic FE model to evaluate the distribution of stresses in a weld-bonded joint which they found to be uniform in the lap zone area. Later on, Chang et al. [8] introduced a 1 mm circular gap around the nugget in the FE simulation of weld-bonded joints. That gap was initiated due to the carbonizing and decomposition of the adhesive layer under continuous electrode heat.

To get an accurate result when FE modeling is used, it is important to include the mechanical properties of both elastic and plastic regions to get an accurate result when FE modeling is used. It is also important for spot welding process to study the microstructure and mechanical properties at nugget and heat affected zone (HAZ) because the plastic properties of the nugget and HAZ are different from the base metal such as in steel [9].

Al-Bahkali et al. [10] built a complete 3D FE modeling of spot welded, adhesive bonded, and weld bonded joints of austenitic stainless steel. Their models are based on elastic-plastic properties, and ductile fracture limit criteria, whereas the adhesive bonding is modeled based on traction separation. They also studied the elastic–plastic properties, fracture limit, nugget and HAZ properties. Furthermore, their load-displacement curves that are obtained from the FE models are compared with the experimental data.

The aim of present work is to study the effect of including the thermal heat caused by spot welding process on the accuracy of representing the load-displacement curves for spot weld, and weld-bonded models for stainless steel (AISI 304).

II. Material Properties Used in Models

The base metal material that was used in the fabrication of the various joints was austenitic stainless steel (AISI 304) annealed condition sheet. This material had the mechanical and thermal properties as shown in Table I. These values were the calculated averages from the standard tensile tests that were performed on three standard samples.

Epoxy adhesive Araldite 2011 was used for bonding to fabricate weld-bonded lap joint specimens. Table I shows also

the mechanical and thermal properties of this adhesive as received by Huntsman Corp. [11]. This adhesive was prepared by the mechanical mixing of equal volumes of resin and hardener. Then, the adhesive was applied and the faying surfaces were placed in their appropriate position (lap joint) after adhesive layer that it was applied using manual rolling, as shown in Fig.1. After rolling, the joints were kept for 2 hours, until the adhesive was slightly hardened and safe for handling. Finally, the joints were cured at 120°C for 60 min to obtain coherent joints.

TABLE I
MATERIAL PROPERTIES OF STRIP, AND ADHESIVE

Material	Adhesive	AISI 304 Steel
Young's Modulus *E*(GPa)	1.90	193.7
Possion's Ratio ν	0.37	0.30
Yield Stress S_y (MPa)	32.0	277.3
Ultimate Stress S_{ut} (MPa)	60.4	729.2
Melting Point (°C)	63.0	1464
Specific heat (J/kg °C)	1667.2	458.5
Thermal expansion (μC^{-1})	60.0	12.0
Thermal conductivity (W/m°K)	0.70	35.0

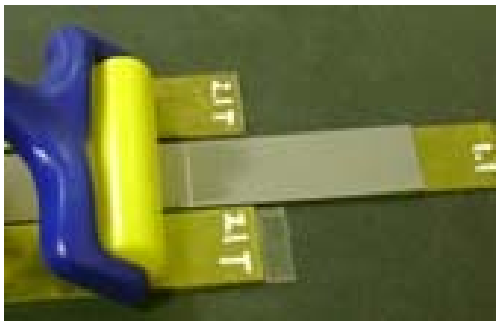

Fig 1 Manual rolling used to make a uniform adhesive layer

The spot welding machine used for the preparation of spot welded specimen joints is Meruit RSW Machine (75kVA). The welding electrodes are water-cooled conical copper alloy electrodes, with contact surface of 4.5mm in diameter. A wooden holder was used, to insure the position of the spot welded joint during welding process as shown in Fig. 2.

Based on the results of many preliminary tests conducted on this material, the welding parameters used to fabricate the spot welded joints are shown in Table II.

TABLE II
WELDING PARAMETERS USED IN SPOT WELDING

Electrode Force (N)	Welding Time sec. (Cycle)	Welding Current (kA)	Heat (%)
600	0.2 (12)	6.5	90

For the weld-bonded specimen joints, the same spot welding parameters are used, except the welding time is increased to become 0.3second (18 cycles) to overcome the effect of adhesive layer. Both models reach a maximum temperature of 1350°C in the nugget area and HAZ during welding process. These values are found to agree with the published results for the same material used by Ghosh and Vivek [12].

Fig 2 Spot welding specimen holder

Spherical indentation is used to define the plastic properties of the nugget and HAZ of AISI 304 steel as shown in Fig. 3. The ductile fracture limits are also defined in term of stress triaxiality and corresponding equivalent strain. This strain is obtained from the tensile test of notched specimen and the stress triaxiality is evaluated using numerical simulation. Consequently, the true stress-true strain curves in these regions were derived using Ahn equation [13].

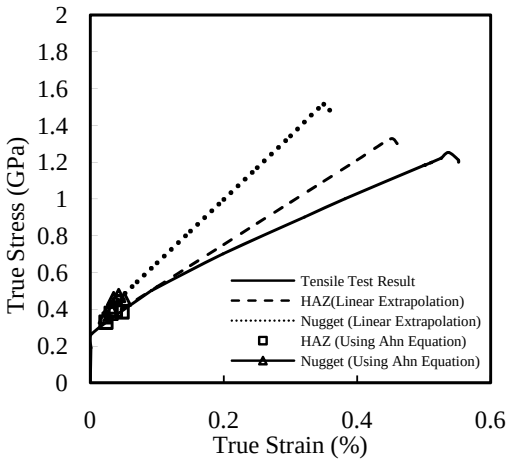

Fig. 3 True stress-true strain curves of the base metal, HAZ, and nugget of spot welded joint for AISI 304 steel

III. FINITE ELEMENT MODELING AND BOUNDARY CONDITIONS

A. Geometric Models

Two different FE models are considered. These models are a single lap spot weld model and a single lap weld-bonded model which are shown in Fig. 4 and Fig. 5 respectively. Each figure shows the configuration, dimensions, constraints and loading conditions. The total length of each model is 175mm and the thickness of each base metal strip is 1mm thicknesses.

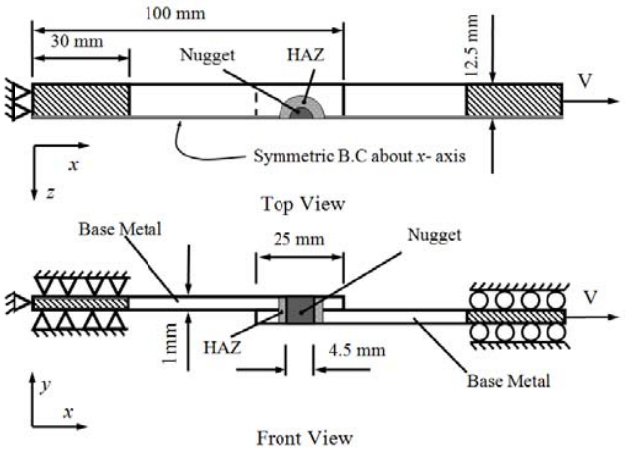

Fig. 4 Spot Weld Model

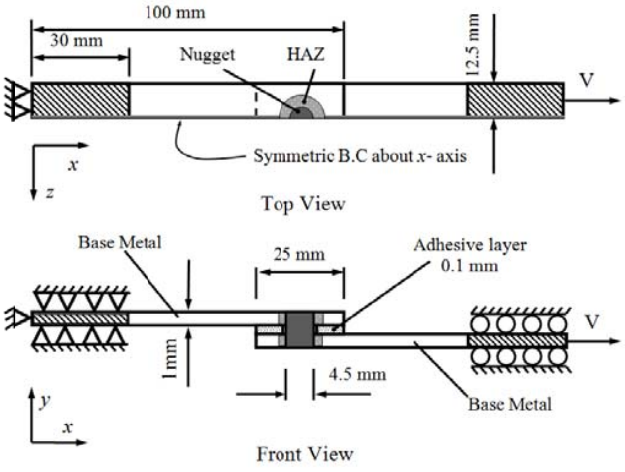

Fig. 5 Weld-Bonded Models

B. Analysis Assumptions

The following assumptions are considered throughout the process: The models are three-dimensional. Half of each model is considered because of symmetry to save computation time. The adhesive layer is isotropic and has a thickness of 0.1mm. There is no adhesive layer in a zone 1 mm around the circumference of the weld nugget and the depth of the indentation assumed to be 0.1 mm for both strips as suggested by Chang et al. [8]. This indentation caused by the electrode of the spot weld machine. All the regions in the FE modelling were connected by sharing nodes. Both models have a started uniform temperature of 1350°C in the nugget area and HAZ. Each model then cools until it reaches the ambient temperature. After that, it is subjected to a tensile force that has a line of action is not initially parallel to the adhesive layer. As the load increases the overlap area bends. Therefore, at the ends of the adhesive layer peel and shear stresses appear. These stresses often induce joint failure.

C. Finite Element Analysis

To find the load-displacement curves for both models, a heat transfer analysis is preformed first to cool the nugget area and HAZ until it reach the ambient temperature. Then, both models are subjected to a tensile force until the joint induced failure. Fig. 6 shows the basic steps in the program simulation algorithm. Where T_i is initial temperature, T_∞ is the ambient temperature, V is the velocity that the model is subjected to at the right edge to simulate the shear tensile test, and h_{air} is the convection heat transfer coefficient.

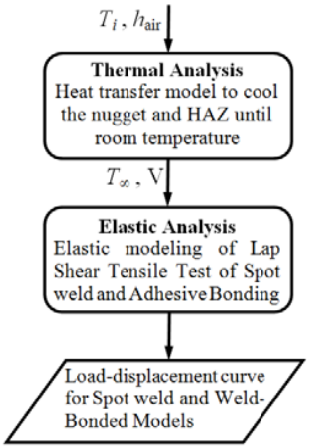

Fig. 6 basic simulation algorithm steps

D. Boundary Conditions

1. Thermal Boundary Conditions

A heat transfer analysis is preformed first to cool the nugget area and HAZ until it reach the ambient temperature. This can be done by considering convection heat transfer only as a thermal boundary condition to be applied at the models surface. Hence, we assume that heat is exchanged with the environment through a convection heat transfer coefficient h_{air} as:

(1)

2. Elastic Boundary Conditions

The mechanical boundary conditions associated with each finite element model can be summarized as the following:

Symmetric boundary conditions is applied along the x-axis side. As a result of that, two constraints are imposed. The rotation and horizontal displacement at the line of symmetry are zero.

On the left edges at x=0, a clamped boundary conditions are imposed. Thus, the displacements become:

(2)

Whereas both strips are subject to a fixed y-direction boundary condition at the beginning 30 mm segment of the

left base metal strip (x=0 to 30mm) and at the end 30mm segment of right base metal strip (x=145 to 175mm).

(3)

In the overlap area a tie constraints are imposed between components of welded joints; i.e. both strips, adhesive layer, and weld nugget. By doing so, the translational and rotational boundary conditions of tied surfaces are made identical, regardless of the way these parts are meshed. The model is subjected to a constant velocity (V=1mm/min.) at the right edges of right base metal strip.

IV. Finite Element Mesh

Finite element computation was carried out using ABAQUS explicit package. Before starting the simulation program and getting results, it is important to specify the element meshes to both models that need to be analyzed to get accurate result in reasonable time. The mesh size must specify based on the ability of representing the variation of the temperature and the mechanical behavior of the model. Thus, the finite-element meshes of these models are generated using eight-node trilinear displacement and temperature, reduced integration with hourglass control (C3D8RT) for the stainless steel (AISI 304) and three dimensional cohesive elements type COH3D8 for the adhesive layer. The numbers of elements for both models that are used in the current study after several refined meshes to insure the conversion of FE results, are given in Table III.

TABLE III
Number of element used in different models

Model	Spot Welded	Weld-Bonded
Base Model Strip	6972	10202
Adhesive Layer	-----	1471
Nugget	690	1035

V. Results

The results of spot weld, and weld-bonded FE simulations including the effect of thermal process (TP) are determined. The results are compared with the same FE models without including the effect of TP and with the experimental results obtained by Al-Bahkali et al. [10].

Stresses resulted from RSW process are very complex due to the combination of high temperature and contact force by electrodes. Fig. 7 shows the contour residual V. Mises stresses after the FE spot welded model undergoes a heat transfer analysis until it reaches ambient temperature from T=1350^{o}C. The maximum stress is 403MPa at the edge of the nugget–strips interface. This residual stress is generated in welded joint as a result of plastic deformation caused by thermal expansion and contraction due to temperature.

Fig. 8 shows the complete load-displacement curves obtained from the FE spot welded modeling results together with the corresponding experimental results obtained from actual spot welded joint. It is clear that both the FE results and the experimental results are in good agreement, except at the plastic region where the model without including TP has an error of 9.2% and for the FE model including TP a small error of 5.2 % is noticed. Both FE models give the same maximum load of 6.94kN, however, the model including TP has more displacement.

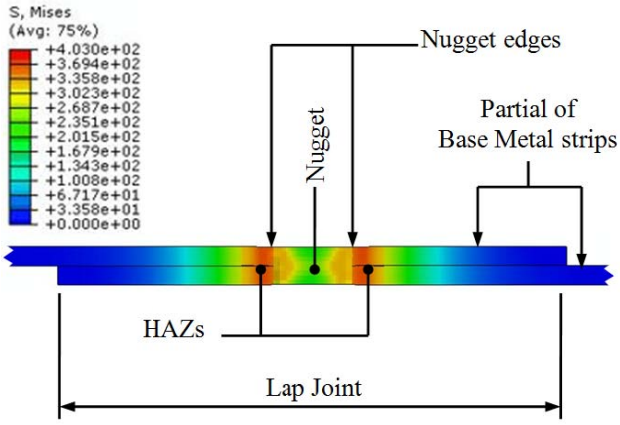

Fig. 7 Contour residual stresses for FE spot welded model

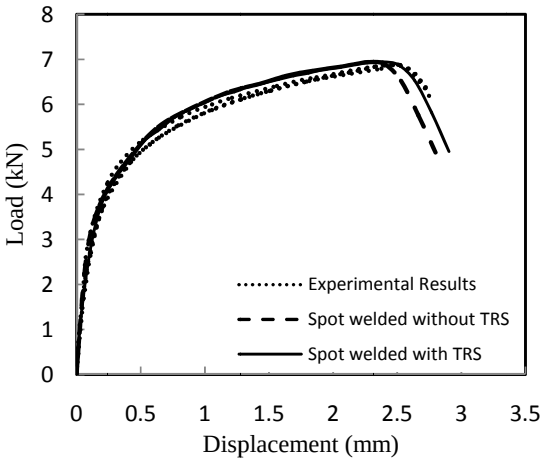

Fig. 8 Load-displacement curves for FE and experimental results of spot welded joints.

Fig. 9 shows the contour residual V. Mises stresses after the FE weld-bonded model undergoes a heat transfer analysis until it reaches ambient temperature from T=1350^{o}C. The maximum stress is 380.5MPa at the edge of the nugget–strips interface.

Fig. 10 shows the complete load-displacement curves obtained from the FE weld-bonded modeling results together with the corresponding experimental results obtained from actual weld-bonded joint. It is clear that both the FE results and the experimental results are in good agreement, except at the plastic region where the model without including TP has an error of 5.6% and for the FE model including TP an error of 6.9 % is noticed. Both FE weld-bonded models give the

same maximum load of 6.94kN. This is because the adhesive layer in weld-bonded joint is failed first.

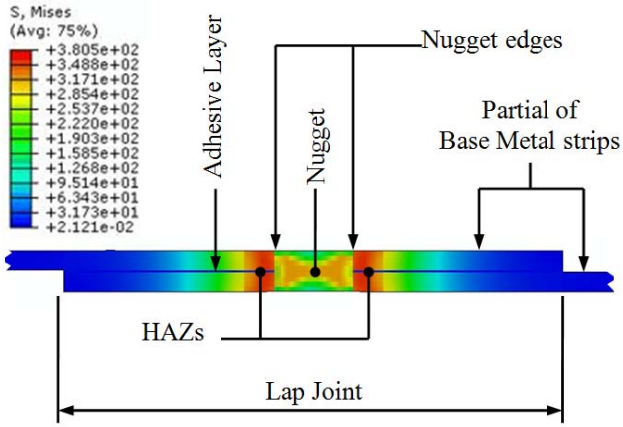

Fig. 9 Contour residual stresses for FE weld-bonded model

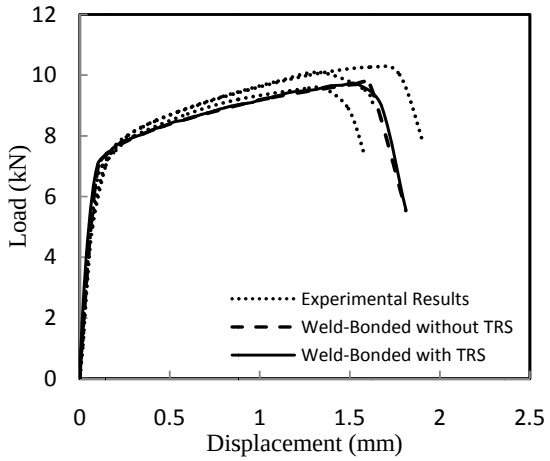

Fig. 10 Load-displacement curves for FE and experimental results of weld-bonded joints.

The results show that for the FE spot welded model, the difference between the model with TP and without in displacement is 4%. In the other hand, for FE weld-bond model, the different between the model with TP and without is less than 1.5%. This is because the failure is first occurs in the adhesive layer.

VI. Conclusion

A three-dimensional FE spot welded and weld-bonded modeling are developed. Both models were first subjected to heat transfer analysis then to an axial load up to the failure point. The knowledge of many properties and quantities such like, the elastic–plastic properties, fracture limit, the properties of the nugget and HAZ are determined. Complete load-displacement curve for each joining model is obtained and compared with the experiment and with the same FE model without including the TP. Adding the effect of TP improved the accuracy of the load-displacement curve for the spot welded model. For the case of weld-boned model, the load-displacement curve for both FE model with or without TP are almost the same. This is because the failure occurs first in the adhesive layer.

References

[1] W. A. Livesey and A. Robinson, "The repair of vehicle bodies," 4th ed., Butterworth-Heinemann, 2000.
[2] J. M. Craddock, "Weld bonding/rivet bonding: Application testing of thin gauge aircraft components," *AIAA*, vol. 73, pp. 805, 1973.
[3] B. Bouyousfi, T. Sahraoui, S. Guessasma, and K. Chaoch, "Effect of process parameter on the physical characteristic of spot weld joints," *Journal of Materials and Design*, vol. 28, pp. 414-419, 2007.
[4] K. Furukawa, M. Katoh, K. Nishio, and T. Yamaguchi, "Influence of electrode pressure and welding conditions on the maximum tensile shear load Q," *Journal of the Japan Welding Society*, pp. 10-16, 2006.
[5] M. N. Cavalli, M. D. Thouless, and Q. D. Yang, "Cohesive-zone modeling of the deformation and fracture of weld-bonded joints," *Welding Journal*, vol. 83, pp. 1335-1395, 2004.
[6] B. Cryns, "Laser weld bonding for aircraft," Insights Edison Welding Institute," 18.2.2, 2005.
[7] B. Chang, Y. Shi and S. Dong, "Comparative studies on stresses in weld-bonded, spot-welded and adhesive-bonded joints," *Journal of Materials Processing Technology*, vol. 87, pp. 230–236, 1999.
[8] B. Chang, Y. Shi, and L. Lu, Studies on studies on stress distribution and fatigue behavior of weld-bonded lap shear joints, *Journal of Materials Processing Technology*, vol. 108, pp. 307–313, 2001.
[9] X. Kong, Q. Yang, B. Li, G. Rothwell, R. English, and H. Ren, "Numerical Study of spot-welded joints of steel," *Journal of Materials and Design*, vol. 29, pp. 1554-1561, 2008.
[10] E. Al-Bahkali, M. Es-Saheb, and J. Herwan, Finite Element Modeling of Weld-Bonded Joint, *The 4th International Conference on Advanced Computational Engineering and Experimenting*, Paris, France, 2010.
[11] Huntsman Corp, "Technical data sheet of structural adhesives araldite-2011," Huntsman Advanced Materials, 2007.
[12] P. K. Ghosh and Vivek, "Weld-bonding of stainless steel," *ISIJ International*, vol. 43, pp. 85-94, 2003.
[13] E. Jeon, J. Y. Kim, M. K. Baik, S. H. Kim, J. S. Park, and D. Kwon, "Optimum definition of true strain beneath a spherical indenter for deriving indentation flow curves", *Journal of Materials Science and Engineering*, Vol. A419, pp. 196-201, 2006.
[14] ABAQUS, User's Manual, Version 6.9, 2010.